Liquid Crystal Phases of Charged Colloidal Platelets

David van der Beek and Henk N. W. Lekkerkerker*

Van 't Hoff Laboratory for Physical and Colloid Chemistry, Debye Institute, Utrecht University, Padualaan 8, 3584 CH, Utrecht, The Netherlands

Received March 2, 2004. In Final Form: May 17, 2004

The liquid crystal phase behavior of a suspension of charged gibbsite [$Al(OH)_3$] platelets is investigated. By variation of the ionic strength, we are able to tune the effective thickness-to-diameter ratio of the platelets in suspension. This enables us to experimentally test the liquid crystal phase transition scenario that was first predicted a decade ago by computer simulations for hard platelets (Veerman, J. A. C.; Frenkel, D. *Phys. Rev. A* **1992**, *45*, 5632), that is, the isotropic (I) to nematic (N) and isotropic to columnar (C) phase transitions in one colloidal suspension. In addition to the shape-dependent thermodynamic driving force, the effect of gravity is important. For example, a biphasic (I−N) suspension becomes triphasic (I−N−C) on prolonged standing. This effect is described by a simple osmotic compression model.

1. Introduction

It has long been known that dispersions of anisotropic colloids display liquid crystal phases. The earliest reports date back to the 1920s and 1930s, when suspensions of rod- and platelike colloids were found to exhibit the isotropic (I) to nematic (N) phase transition. Some notable examples include rodlike vanadium pentoxide (V_2O_5)[1] and tobacco mosaic virus[2] particles and platelike clay particles observed by Langmuir[3] in 1938.

In retrospect, observing the I−N transition in suspensions of rod- and platelike colloids is not very surprising. Already in the 1940s, just a few years after the mentioned experiments and actually inspired by them, Lars Onsager proposed an explanation for the I−N transition on purely entropic grounds:[4,5] the competition between packing entropy (which favors the nematic state) and orientational entropy (favoring the isotropic state) determines the I−N phase behavior. As the packing entropy becomes more important at higher volume fractions, the particles tend to align and form a nematic phase at high enough concentration. Onsager also showed that particle shape alone is enough to induce such behavior. Thus, even hard rods or plates without any interaction may form a nematic phase. This notion was confirmed by computer simulations.[6,7]

Veerman and Frenkel[8] found that hard platelets may also form a columnar (C) phase. In addition to the mere existence of the columnar phase, these authors found that systems of platelets show either the I−N and subsequently the N−C transition or directly the I−C phase transition, depending on the thickness-to-diameter ratio (aspect ratio). Quite recently, these two scenarios have been observed experimentally. The first scenario was reported to occur in a suspension of sterically stabilized gibbsite platelets[9,10] whereas the second was observed in a suspension of charged nickel hydroxide [$Ni(OH)_2$] platelets.[11] The aspect ratio was 1/11 in the first case and 1/5 in the second, and, hence, the observed scenarios are in agreement with the computer simulations.

Still, there is one issue to be resolved: the different scenarios have never been observed in one colloidal system. In this report, we show that this can be achieved in systems of charge-stabilized colloidal gibbsite platelets by variation of the ionic strength. This study is an extension to an earlier one in which, for the first time since Langmuir, I−N phase separation in a suspension of charged platelets was observed.[12] Our results can be understood on the basis of the phase diagram of Veerman and Frenkel.[8] In addition, we have found that gravity plays a major role on the phase behavior of our platelet suspensions, like in the case of colloidal spheres[13−17] and rods.[18−21] Our results are described by a simple osmotic compression model that we developed.

2. Experiment

2.1. Preparation and Characterization. The suspension of gibbsite platelets was synthesized following a modified version of a procedure that was developed earlier at our laboratory.[9,22] To a solution of HCl (2 L, 0.09 M) aluminum *sec*-butoxide (0.08 M, Fluka Chemika, pract. >95%) and aluminum isopropoxide (0.08 M, Acros Organics, 98+%) were added. It was stirred for 17 days and subsequently heated for 65 h at 85 °C in a polypropylene vessel by means of a waterbath. The resulting turbid suspension was dialyzed for 11 days against demineralized

* To whom correspondence should be addressed. E-mail: h.n.w.lekkerkerker@chem.uu.nl. Phone: +31 (0)30 253 2547. Fax: +31 (0)30 253 3870.

(1) Zocher, H. *Z. Anorg. Chem.* **1925**, *147*, 91.
(2) Bawden, F. C.; Pirie, N. W.; Bernal, J. D.; Fankuchen, I. *Nature* **1936**, *138*, 1051.
(3) Langmuir, I. *J. Chem. Phys.* **1938**, *6*, 873.
(4) Onsager, L. *Phys. Rev.* **1942**, *62*, 558.
(5) Onsager, L. *Ann. N.Y. Acad. Sci.* **1949**, *51*, 627.
(6) Vieillard-Baron, J. *Mol. Phys.* **1974**, *28*, 809.
(7) Frenkel, D.; Eppenga, R. *Phys. Rev. Lett.* **1982**, *49*, 1089.
(8) Veerman, J. A. C.; Frenkel, D. *Phys. Rev. A* **1992**, *45*, 5632.
(9) van der Kooij, F. M.; Lekkerkerker, H. N. W. *J. Phys. Chem. B* **1998**, *102*, 7829.
(10) van der Kooij, F. M.; Kassapidou, K.; Lekkerkerker, H. N. W. *Nature* **2000**, *406*, 868.
(11) Brown, A. B. D.; Clarke, S. M.; Rennie, A. R. *Langmuir* **1998**, *14*, 3129.
(12) van der Beek, D.; Lekkerkerker, H. N. W. *Europhys. Lett.* **2003**, *61*, 702.
(13) Crandall, R. S.; Williams, R. *Science* **1977**, *198*, 293.
(14) Hachisu, S.; Takano, K. *Adv. Colloid Interface Sci.* **1982**, *16*, 233.
(15) Piazza, R.; Bellini, T.; Degiorgio, V. *Phys. Rev. Lett.* **1993**, *71*, 4267.
(16) Rutgers, M. A.; Dunsmuir, J. H.; Xue, J.-Z.; Russel, W. B.; Chaikin, P. M. *Phys. Rev. B* **1996**, *53*, 5043.
(17) Sullivan, M.; Zhao, K.; Harrison, C.; Austin, R. H.; Megens, M.; Hollingsworth, A.; Russel, W. B.; Cheng, Z.; Mason, T.; Chaikin, P. M. *J. Phys.: Condens. Matter* **2003**, *15*, S11.
(18) Oster, G. *J. Gen. Physiol.* **1950**, *33*, 445.
(19) Kreibig, U.; Wetter, C. *Z. Naturforsch., C: Part. Fields* **1980**, *35*, 750.
(20) Brian, A. A.; Frisch, H. L.; Lerman, L. S. *Biopolymers* **1981**, *20*, 1305.
(21) Baulin, V. A.; Khokhlov, A. R. *Phys. Rev. E* **1999**, *60*, 2973.
(22) Wierenga, A. M.; Lenstra, T. A. J.; Philipse, A. P. *Colloids Surf., A* **1998**, *134*, 359.

10.1021/la049455i CCC: $27.50
Published on Web 07/09/2004

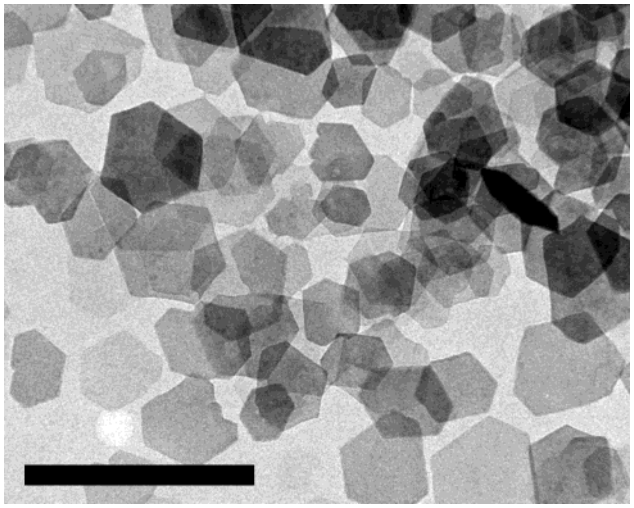

Figure 1. Transmission electron micrograph of the hexagonal gibbsite platelets used in this study. The scale bar denotes 500 nm.

water to get rid of excess reactants and byproducts. The gibbsite content was determined to be 6.8 g/L.

It has been observed that the presence of Al_{13} ions [$Al_{13}O_4(OH)_{24}(H_2O)_{12}^{7+}$] has a stabilizing effect on suspensions of colloidal boehmite particles.[23−27] Furthermore, Hernandez[28] presented a systematic study of the adsorption of aluminum polycations, in particular Al_{13}, on colloidal iron and aluminum oxyhydroxides and hydroxides (i.e., gibbsite particles). He used ^{27}Al NMR to study the reaction of the Al_{13} species with the surface of these particles. He concluded that the adsorption leads to an increased surface charge, which in turn appears to enhance the stability of the particles. In view of this, we used Al_{13} ions (as produced by hydrolysis of aluminum chlorohydrate,[24] $Al_2(OH)_5Cl{\cdot}2-3H_2O$) to stabilize our gibbsite platelets. To 200 mL of gibbsite dispersion (as obtained from the synthesis), 1.0 g of aluminum chlorohydrate was added. This mixture was shaken vigorously for 1.5 min, after which it was put away at room temperature for 3 days. Through a sequence of sedimentation (20 h, 1400 G) and redispersion, excess Al_{13} was removed and sodium chloride added to bring the suspensions to the intended ionic strength, either 0.1, 1, or 10 mM. Measurements showed that the conductivity was close to that of the stock NaCl solutions.

From the gibbsite dispersion, a sample was taken for investigation with transmission electron microscopy (TEM) by dipping a coated copper grid in a very dilute suspension. The electron microscope was equipped with a charge-coupled device camera that was used to take micrographs. From such micrographs, as depicted in Figure 1, the average particle diameter (defined as the average of the average corner-to-corner distances) was obtained using image analysis software. The anisotropic particle shape allowed us to determine the thickness of the platelets to within 0.1 nm using atomic force microscopy (AFM). Obviously, the *effective* particle dimensions in suspension depend strongly on the ionic strength; this issue will be addressed further on. The particle characteristics are listed in Table 1.

2.2. Samples and Methods. To study the phase behavior of our dispersions, weighed amounts of stock dispersion were put in spectrophotometric cells (2 mm). The stock-particle concentration was determined by drying a known amount of dispersion at 75 °C to constant weight. Variation of particle concentration in the cells was achieved by diluting with sodium chloride solution or by centrifugation, removal of supernatant, and redispersion. After thorough homogenization, the samples were stored at room temperature to reach phase equilibrium. Once phase-separated, the samples were checked for liquid crystallinity with crossed polarizers.

Table 1. Characteristics of the Colloidal Platelets Used in This Study, As Obtained by TEM (for the diameter $\langle D \rangle$) and AFM (for the thickness $\langle L \rangle$)[a]

$\langle D \rangle$	202 nm	$\langle L \rangle$	13.2 nm
σ_D	38 nm (19%)	σ_L	3.6 nm (27%)
$\langle D \rangle / \langle L \rangle$	15.3		

[a] The given dimensions refer to the particle core; σ_D and σ_L express polydispersities.

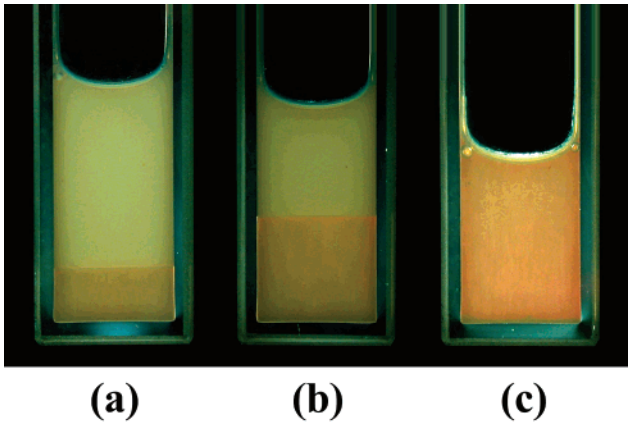

Figure 2. I−N phase transition observed between crossed polarizers. The ionic strength in these samples is 10 mM and the gibbsite concentrations are (a) 328, (b) 356, and (c) 464 g/L. Sample c is well into the nematic phase, in contrast with our earlier study[12] where gelation impeded the formation of a completely nematic phase.

3. Results and Discussion

3.1. Phase Behavior As Determined by Salt Concentration. At an ionic strength of 10 mM NaCl, the suspensions are isotropic at gibbsite concentrations up to about 259 g/L. Between crossed polarizers, only flow birefringence is observed. However, on increasing the particle concentration to above the mentioned value the suspensions become permanently birefringent. On a time scale of 24 h, they separate into two distinct layers divided by a sharp interface. The birefringent bottom layer appears to be a nematic phase in equilibrium with the isotropic upper phase. This isotropic phase shows very strong flow birefringence with a decay time of about 0.3 s. The nematic phase shows a threaded texture that is very typical of a nematic phase.[29] The relative amount of nematic phase increases with increasing particle concentration; see Figure 2. In contrast with earlier observations,[12] the samples now become fully nematic, around 409 g/L. On increasing the concentration even further, gelation is observed instead of the expected N−C phase transition. Apparently, gelation still cannot be avoided when concentrating in the usual way. However, by letting gravity work on our suspension, we have been able to induce a high particle concentration in a very gentle way. This is described in more detail in the next section.

At somewhat lower ionic strength (1.9 and 1.4 mM), the suspensions also show the I−N phase transition. However, when going to even lower ionic strength (1 mM and below), the nematic phase is not observed anymore. Suspensions at 1 and 0.1 mM NaCl show an isotropic phase at low

(23) Bugosh, J. *J. Phys. Chem.* **1961**, *65*, 1789.
(24) van Bruggen, M. P. B.; Donker, M.; Lekkerkerker, H. N. W.; Hughes, T. L. *Colloids Surf., A* **1999**, *150*, 115.
(25) Ramsay, J. D. F.; Daish, A. R.; Wright, C. J. *J. Chem. Soc., Faraday Discuss.* **1978**, *65*, 65.
(26) Drouin, J. M.; Chopin, T.; Nortier, P.; van Damme, H. *J. Colloid Interface Sci.* **1987**, *125*, 314.
(27) Beattie, J. K.; Cleaver, J. K.; Waite, T. D. *Colloids Surf., A* **1996**, *111*, 131.
(28) Hernandez, J. Thèse de Doctorat de l'Université Pierre et Marie Curie, Université Pierre et Marie Curie, Paris, France, 1998.
(29) de Gennes, P. G. *The Physics of Liquid Crystals*; Clarendon Press: Oxford, 1974.

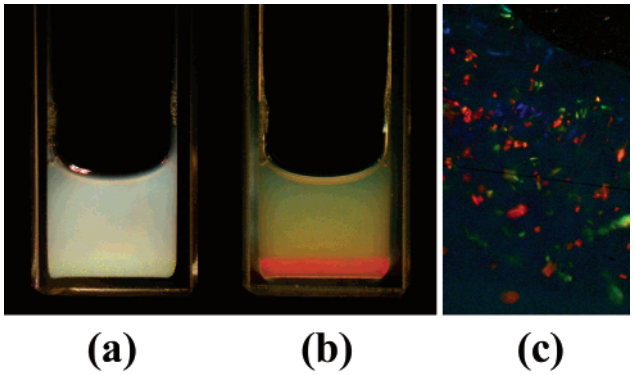

Figure 3. Phase-separated sample in I−C equilibrium, (a) illuminated by white light and (b) between crossed polarizers. Part c depicts a close-up of the Bragg reflections in another columnar sample. The Bragg reflections stem from the two-dimensional hexagonal lattice of columns of platelets, with a lattice spacing of about 200 nm.

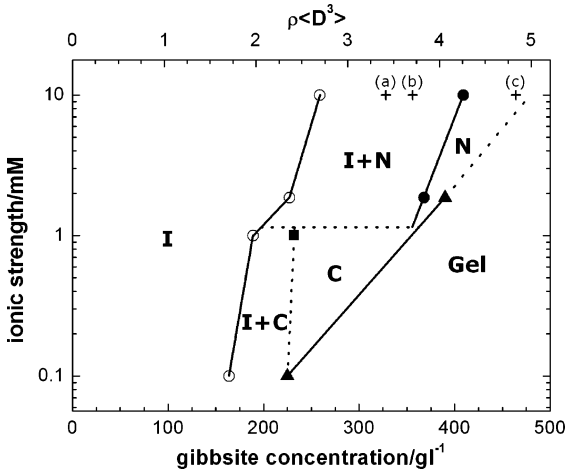

Figure 4. Experimental phase diagram of the gibbsite suspension. Boundaries between the phase regions are indicated with lines. Dashed lines indicate tentative phase boundaries. The plus signs and accompanying characters refer to the samples in Figure 2.

gibbsite concentration (<170 g/L) and I−C phase separation on increasing particle concentration. The columnar phase is easily identified by the presence of Bragg reflections; see Figure 3. The relative amount of the columnar phase increases with increasing particle concentration, up to the point where the samples become fully columnar (1 mM) or gel (0.1 mM). All observations are depicted in a phase diagram, Figure 4. Note that the slope of the sol−gel line is opposite to that of clay suspensions studied earlier.[30−32] Apparently, as opposed to these clays, in our suspensions repulsion dominates the interparticle interactions. Levitz et al.[33] find similar behavior in Laponite suspensions at very low ionic strength.

To compare our results with other ones, it is necessary to express our mass concentrations in dimensionless number densities (ND^3/V). It can easily be shown that the volume fraction ϕ of monodisperse hexagonal platelets in solution equals

$$\phi = \rho\frac{3}{8}\sqrt{3}D^2L \tag{1}$$

with D and L being the diameter and thickness of the particle, respectively, and $\rho = N/V$ being the number density. For polydisperse particles, eq 1 becomes

$$\phi_{\mathrm{pol}} = \rho\frac{3}{8}\sqrt{3}\langle D^2L\rangle = \rho\frac{3}{8}\sqrt{3}\frac{\langle D^2L\rangle}{\langle D^3\rangle}\langle D^3\rangle \tag{2}$$

Following van der Kooij and co-workers,[34] we assume that D and L are uncorrelated and that the particle diameter distribution is symmetric, so $\langle D^3\rangle/\langle D\rangle^3 = 1 + 3\sigma_D^2$ and $\langle D^2\rangle/\langle D\rangle^2 = 1 + \sigma_D^2$ with σ being the diameter polydispersity. This yields

$$\phi_{\mathrm{pol}} = \frac{3}{8}\sqrt{3}\frac{\langle L\rangle}{\langle D\rangle}\frac{1+\sigma_D{}^2}{1+3\sigma_D{}^2}\rho\langle D^3\rangle \tag{3}$$

which in turn can be rewritten as

$$\rho\langle D^3\rangle = \frac{8}{9}\sqrt{3}\frac{\langle D\rangle}{\langle L\rangle}\frac{1+3\sigma_D{}^2}{1+\sigma_D{}^2}\phi_{\mathrm{pol}} \tag{4}$$

The (core) volume fraction is related to the mass concentration through the mass density of gibbsite (2420 kg/m^3). In our suspensions, the I−N phase transition occurs between 259 and 409 g/L, yielding dimensionless densities of $\rho_{\mathrm{iso}}D^3 = 2.7$ and $\rho_{\mathrm{nem}}D^3 = 4.3$. Table 2 shows our results in comparison with that of other experimental[9] and theoretical[35] work and computer simulations.[36,37] Because the I−N phase transition is driven by the excluded volume, electrostatic effects are of crucial importance. However, in the comparison with other work only number densities were needed, which can be obtained from our results without considering the electrostatic effects.

As stated earlier, the main issue of this paper is the observation of two different regimes in one suspension. At relatively high ionic strength, the I−N phase transition is observed, while at low ionic strength, the I−C transition occurs. This can be understood on the basis of the phase diagram of Veerman and Frenkel, obtained by Monte Carlo (MC) computer simulations.[8] They studied cut spheres as a model system for hard platelets and found the I−N transition occurring for aspect ratios smaller than $L/D =$

Table 2. Comparison of the I−N Phase Transition Densities of Our Suspension with Those of Other Studies

ref	method	$\rho_{\mathrm{iso}}\langle D^3\rangle$	$\rho_{\mathrm{nem}}\langle D^3\rangle$
36, 37	MC with hard platelets, 19% polydisperse[a]	3.2	4.0
9	experiment with hard platelets	2.5	2.7
35	theory on charged Laponite clay platelets	3.2	
this study	experiment with charged platelets at 10 mM	2.7	4.3

[a] From MC computer simulations, phase transition densities were found for monodisperse hexagonal disks[36] and polydisperse circular disks.[37] Following Bates,[36] we find $\rho_{\mathrm{iso}}D^3 = 3.2$ and $\rho_{\mathrm{nem}}D^3 = 4.0$ as an estimate for 19% polydisperse hexagonal disks.

(30) Mourchid, A.; Delville, A.; Lambard, J.; Lécolier, E.; Levitz, P. *Langmuir* **1995**, *11*, 1942.
(31) Gabriel, J. C. P.; Sanchez, C.; Davidson, P. *J. Phys. Chem.* **1996**, *100*, 11139.
(32) Mourchid, A.; Lécolier, E.; Van Damme, H.; Levitz, P. *Langmuir* **1998**, *14*, 4718.
(33) Levitz, P.; Lécolier, E.; Mourchid, A.; Delville, A.; Lyonnard, S. *Europhys. Lett.* **2000**, *49*, 672.
(34) van der Kooij, F. M.; van der Beek, D.; Lekkerkerker, H. N. W. *J. Phys. Chem. B* **2001**, *105*, 1696.
(35) Rowan, D. G.; Hansen, J. P. *Langmuir* **2002**, *18*, 2063.
(36) Bates, M. A. *J. Chem. Phys.* **1999**, *111*, 1732.
(37) Bates, M. A.; Frenkel, D. *J. Chem. Phys.* **1999**, *110*, 6553.

1/7, while the I−C transition occurred for ratios larger than $L/D = 1/7$. Our charged particles are not hard platelets; still we can map them on a hard platelet system by introducing an *effective* diameter and *effective* thickness, a notion that goes back to Onsager himself.[4,5] In such a description, the effective diameter of a platelet can be regarded as the core dimension plus some constant times the Debye length. Let us assume that this holds for the thickness as well and that the constant is the same for the diameter and thickness. In that case

$$L^{\text{eff}} = L^{\text{core}} + a\kappa^{-1} \tag{5a}$$

$$D^{\text{eff}} = D^{\text{core}} + a\kappa^{-1} \tag{5b}$$

where a is the constant to be determined and κ^{-1} is the Debye length. From Figure 4, our experimental phase diagram, it appears that the ionic strength at the changeover is 1.2 ± 0.2 mM, which corresponds to a Debye length of 9.1 nm. The effective aspect ratio $L^{\text{eff}}/D^{\text{eff}}$ at the changeover must be 1/7. Together with the core dimensions from Table 1 and eq 5, this yields $a = 2.0$. In other words, the interparticle distance at which two platelets presumably have a repulsion of about kT is 2.0 times the Debye length, which agrees with the value that Stroobants and co-workers found for charged rods,[38] that is, $a = 2.9$.

However, this hard platelet picture falls short. The core volume fractions at which the I−C phase transition occurs (at 1.2 mM) are $\phi_{\text{I}}^{\text{core}} = 0.08$ and $\phi_{\text{C}}^{\text{core}} = 0.10$. It can easily be shown that the *effective* volume fraction is related to the *core* volume fraction as follows:

$$\phi^{\text{eff}} = \frac{L^{\text{eff}}}{L^{\text{core}}}\left(\frac{D^{\text{eff}}}{D^{\text{core}}}\right)^2 \phi^{\text{core}} \tag{6}$$

where we now explicitly use superscripts. (Note that in eqs 1−4, the core volume fraction is used although this is not explicitly mentioned.) The effective volume fractions consequently are $\phi_{\text{I}}^{\text{eff}} = 0.22$ and $\phi_{\text{C}}^{\text{eff}} = 0.26$. These values should be compared with $\phi_{\text{I}} \simeq 0.45$ and $\phi_{\text{C}} \simeq 0.50$ that follow from the simulations of Veerman and Frenkel.[8] Clearly, the soft repulsive tail of the electric double layer between the platelets lowers the effective volume fractions at which the I−C transition occurs.

3.2. Phase Behavior As Determined by Gravity. As mentioned before, the suspensions at 10 mM become fully nematic, but the columnar phase does not show up at this ionic strength because of gelation. However, by letting gravity act on our suspensions, we have been able to induce a high particle concentration in a very gentle way, avoiding the formation of a gel. A sample containing an isotropic and a nematic phase in coexistence (in a 60:40% ratio) was left at room temperature to observe the effect of gravity. After 6 months, we found that the sample contained three phases instead of the initial two, the upper two phases being isotropic and nematic, respectively, whereas the lower phase appeared to be columnar; see Figure 5. This columnar phase shows a grainy texture and bright Bragg reflections due to the two-dimensional positional order. The measured relative heights of the phases are listed in Table 3. Close inspection of the sample reveals a particle concentration gradient as a function of height, indicating a balance between gravity and osmotic pressure. Using a simple model, developed in cooperation with Wensink,[39] this balance and the resulting three-phase equilibrium can be described qualitatively.

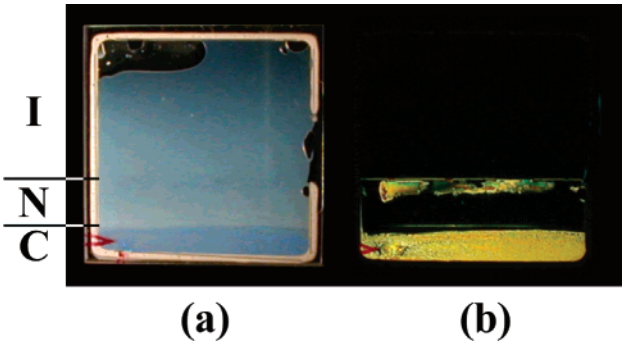

Figure 5. Initially biphasic (I−N) sample that developed a third phase (C) on a time scale of six months. Part a depicts the sample at ordinary illumination, and part b depicts that between crossed polarizers. Again, Bragg reflections can be observed in the columnar phase; see part a. In part b, the major part of the nematic phase appears dark; this is because of the alignment of the platelets along the wall (homeotropic alignment).

Table 3. Relative Heights of the Phases in the Sample in Sedimentation Equilibrium, As Measured in Our Experiment and Calculated with the Osmotic Compression Model

	experiment	model
I	0.61	0.54
N	0.21	0.13
C	0.18	0.33

For a monodisperse system of colloidal particles with buoyant mass m^* and number density ρ, the equilibrium condition reads

$$-\frac{\partial \Pi}{\partial z} = m^* g \rho \tag{7}$$

where z denotes the vertical position in the sample. Equation 7 is easily rewritten into

$$-\left(\frac{\partial \Pi}{\partial \rho}\right)\frac{\partial \rho}{\partial z} = m^* g \rho \tag{8}$$

in terms of the osmotic compressibility $(\partial\Pi/\partial\rho)$. For the sake of universality, we introduce the reduced quantities $\tilde{\Pi} = \Pi D^3/k_{\text{B}}T$, $\xi = k_{\text{B}}T/m^*g$, and $c = \rho D^3$ and substitute eq 8, yielding

$$\frac{1}{c}\left(\frac{\partial \tilde{\Pi}}{\partial c}\right) \mathrm{d}c = -\frac{\mathrm{d}z}{\xi} \tag{9}$$

The height $H = z_{\text{top}} - z_{\text{bottom}}$ of a single phase is obtained by integrating eq 9 with corresponding boundaries c_{top} and c_{bottom} (the reduced platelet densities at the top and bottom of the phase, respectively), resulting in

$$\frac{H}{\xi} = -\int_{c_{\text{bottom}}}^{c_{\text{top}}} \frac{1}{c}\frac{\partial \tilde{\Pi}}{\partial c}\,\mathrm{d}c \tag{10}$$

Furthermore, the average concentration $\bar{c}$ in the phase equals

$$H\bar{c} = \int_{z_{\text{bottom}}}^{z_{\text{top}}} c(z)\,\mathrm{d}z = \int_{c_{\text{bottom}}}^{c_{\text{top}}} c(z)\frac{\mathrm{d}z}{\mathrm{d}c}\,\mathrm{d}c \tag{11}$$

Substituting with eq 9, this yields

$$H\bar{c} = -\xi\int_{c_{\text{bottom}}}^{c_{\text{top}}} \frac{\partial \tilde{\Pi}}{\partial c}\,\mathrm{d}c = \xi[\tilde{\Pi}(c_{\text{bottom}}) - \tilde{\Pi}(c_{\text{top}})] \tag{12}$$

This result simply expresses hydrostatic equilibrium in

(38) Stroobants, A.; Lekkerkerker, H. N. W.; Odijk, T. *Macromolecules* **1986**, *19*, 2232.

(39) Wensink, H. H.; Lekkerkerker, H. N. W. *Europhys. Lett.* **2004**, *66*, 125.

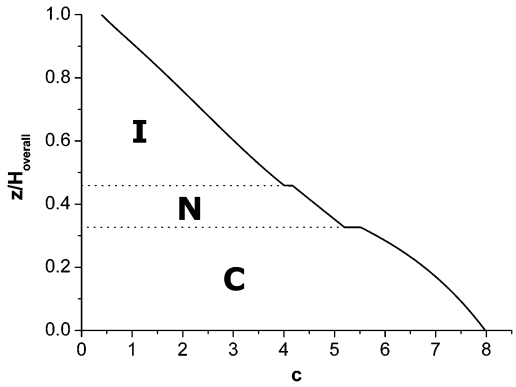

Figure 6. Sedimentation profile (relative height vs concentration) that was calculated using the osmotic compression model. The overall concentration was set to $c = 4.1$ (in the I−N biphasic gap) as dictated by the experiment.

which the difference in osmotic pressure above and below a layer is balanced by the weight of the layer. The relations that we have derived for a single phase (eqs 10 and 12) now apply to each of the phases in a multiphase equilibrium. For our case of an isotropic, nematic, and columnar phase, we find for the individual heights

$$\frac{H_I}{\xi} = -\int_{c_{IN}}^{c_{top}} \frac{1}{c}\frac{\partial \tilde{\Pi}_I}{\partial c}\,dc \tag{13a}$$

$$\frac{H_N}{\xi} = -\int_{c_{NC}}^{c_{NI}} \frac{1}{c}\frac{\partial \tilde{\Pi}_N}{\partial c}\,dc \tag{13b}$$

$$\frac{H_C}{\xi} = -\int_{c_{bottom}}^{c_{CN}} \frac{1}{c}\frac{\partial \tilde{\Pi}_C}{\partial c}\,dc \tag{13c}$$

where in each case the integration boundaries are the concentrations at the top and bottom of the phase under consideration. Again, the average concentration in each phase is given by

$$H_I\bar{c}_I = \xi[\tilde{\Pi}(c_{IN}) - \tilde{\Pi}(c_{top})] \tag{14a}$$

$$H_N\bar{c}_N = \xi[\tilde{\Pi}(c_{NC}) - \tilde{\Pi}(c_{NI})] \tag{14b}$$

$$H_C\bar{c}_C = \xi[\tilde{\Pi}(c_{bottom}) - \tilde{\Pi}(c_{CN})] \tag{14c}$$

Interestingly, this result allows for further analysis. Obviously,

$$H_{overall} = H_I + H_N + H_C \tag{15}$$

and

$$H_{overall}\bar{c}_{overall} = H_I\bar{c}_I + H_N\bar{c}_N + H_C\bar{c}_C \tag{16}$$

From coexistence theory, we know that

$$\tilde{\Pi}(c_{IN}) = \tilde{\Pi}(c_{NI}) \tag{17a}$$

$$\tilde{\Pi}(c_{NC}) = \tilde{\Pi}(c_{CN}) \tag{17b}$$

Substituting these in eq 16 and making use of eq 14, we find that

$$H_{overall}\bar{c}_{overall} = \xi[\tilde{\Pi}(c_{bottom}) - \tilde{\Pi}(c_{top})] \tag{18}$$

just like the case of one phase. This equation, together with eqs 13 and 15, allows for explicit calculation of c_{top} and c_{bottom} and, hence, the sedimentation profile once the equation of state (EOS) is known. For charged platelets, no EOS is known. However, a hard-platelet EOS was given by Zhang and co-workers[40] for platelets with an aspect ratio of 0.10. We take this EOS for a qualitative approach to the problem, resulting in a calculated sedimentation profile that is shown in Figure 6 and the corresponding phase heights in Table 3. Apparently, this approach describes the sample reasonably well.

4. Conclusion

We have studied the phase behavior of charged colloidal gibbsite platelets by observing the effects of varying ionic strength and gravity. Through variation of the ionic strength, we have been able to tune the effective aspect ratio of the platelets. This enabled us to observe both the I−N and I−C phase transition in one suspension, a scenario predicted by MC computer simulations a decade ago.

The effect of gravity is quite important. A biphasic (I−N) sample became triphasic (I−N−C) after standing for several months, which is described by a simple osmotic compression model that we developed.

Acknowledgment. We thank H. H. Wensink for helpful discussions on the osmotic compression model.

LA049455I

(40) Zhang, S.-D.; Reynolds, P. A.; van Duijneveldt, J. S. *J. Chem. Phys.* **2002**, *117*, 9947.